Empirical Estimation of Nearshore Waves From a Global Deep-Water Wave Model

Matthew Browne, Darrell Strauss, Bruno Castelle, Michael Blumenstein, Rodger Tomlinson, and Chris Lane

***Abstract*—Global wind-wave models such as the National Oceanic and Atmospheric Administration WaveWatch 3 (NWW3) play an important role in monitoring the world's oceans. However, untransformed data at grid points in deep water provide a poor estimate of swell characteristics at nearshore locations, which are often of significant scientific, engineering, and public interest. Explicit wave modeling, such as the Simulating Waves Nearshore (SWAN), is one method for resolving the complex wave transformations affected by bathymetry, winds, and other local factors. However, obtaining accurate bathymetry and determining parameters for such models is often difficult. When target data is available (i.e., from *in situ* buoys or human observers, empirical alternatives such artificial neural networks (ANNs) and linear regression may be considered for inferring nearshore conditions from offshore model output. Using a sixfold cross-validation scheme, significant wave height H_s and period were estimated at one onshore and two nearshore locations. In estimating H_s at the shoreline, the validation performance of the best ANN was $r = 0.91$, as compared to those of linear regression (0.82), SWAN (0.78), and the NWW3 H_s baseline (0.54).**

***Index Terms*—Artificial neural networks (ANNs), National Oceanic and Atmospheric Administration (NOAA) WW3 (NWW3), nearshore, waves, WaveWatch 3 (WW3).**

I. Introduction

KNOWLEDGE of swell conditions at specific nearshore locations is often important for research, marine engineering, and policy development. Although global swell models are an effective approximation of open swell conditions, they often become less accurate in the nearshore zone. Variations in nearshore bathymetry, local wind-generated seas, and the effects of artificial structures transform deep-water swell due to reflection, shoaling, refraction, diffraction, and breaking [1]. At a particular location, local topography may lead to attenuation or accentuation of long- or short-period swells, either directly or by the contribution of local wind conditions.

The propagation of swell in nearshore areas is conventionally studied by running either an actual or a virtual simulated physical model [1]. Physical-scale models require a significant investment of resources for their construction and simulation. For this reason, numerical computer simulation of the local physical environment and local swell conditions is often preferred. However, numerical models themselves require care and expertise in their implementation, typically along with days of processing time, and produce results that are sometimes unsatisfactory, especially in shallow water. These techniques are also sensitive to the accuracy of the bathymetric data for the study area.

Physical wave recordings and observations are used to calibrate and validate theoretical [2] and empirical [3], [4] approaches to modeling the wave transformations that occur as they progress from deep to shallow water. The method of [4], for instance, was based on comparisons between buoy-measured H_s in deep water and visual observations of trough-to-crest vertical wave height at the break point at nearby locations.

Artificial neural networks (ANNs) (discussed in Section I-B) should be regarded as a further extension of empirical (i.e., statistical curve fitting to large numbers of observations), as opposed to model-based, attempts to estimate and predict wave behavior [5]. The use of ANNs has been reported for numerous applications in the geological and marine sciences and, in particular, have been used in forecasting wave climate time series [6]–[8]. ANNs have been applied to estimating missing wave-buoy data [9], and recently, Kalra *et al.* [10] has detailed an ANN-based effort to map offshore wave data to coastal locations. Apart from Kalra *et al.*'s [10] welcome comparison of ANN performance with that of linear regression, most research has not compared ANNs with other forms of swell estimation. As neural networks are unconstrained general-purpose-function approximators with potentially thousands of degrees of freedom, some questions exist regarding the validity of previous works.[1] An empirical approach does not provide the insight into wave propagation processes that is provided by full-scale numerical modeling. However, the advantages include computational efficiency and potentially greater predictive power, without the need for detailed geographic information or the laborious testing of a range of physical model parameters.

This letter aims to estimate significant wave height H_s at the shore and two nearshore locations using the input from the National Oceanic and Atmospheric Administration WaveWatch 3 (NWW3). Nonlinear ANNs of varying complexity are compared with the baseline H_s recorded by the global model, a linear predictor, and the spectral wave model Simulating Waves Nearshore (SWAN). Combined with a k-fold cross-validation

Manuscript received August 11, 2005; revised January 11, 2006. This work was supported by an Australian Research Council Grant.

M. Browne, D. Strauss, B. Castelle, and R. Tomlinson are with the Griffith University Centre for Coastal Management, Brisbane 4111, Australia (e-mail: m.browne@griffith.edu.au).

M. Blumenstein is with the School of Information and Communication Technology, Griffith University, Brisbane 4111, Australia.

C. Lane is with CoastalWatch Technologies, Surfers Paradise, Queensland, Australia.

Digital Object Identifier 10.1109/LGRS.2006.876225

[1]For example, a method of wave forecasting using neural networks was recently reported in [11] and subsequently, challenged [12] due to issues related to overfitting, lack of baseline performance comparisons, and an insufficient degree of cross validation.

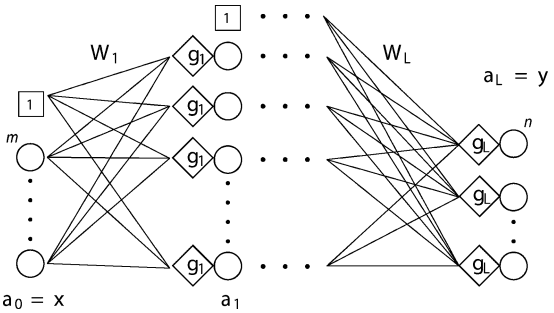

Fig. 1. Standard feedforward ANN architecture.

experimental setup, this approach ought to resolve the efficacy of neural networks for the interesting task of bringing global ocean wave model output to nearshore locations. A practical outcome is that the NWW3 output may be utilized inexpensively for the emulation or prediction of surf reporter or buoy readings at locations of interest.

A. SWAN

SWAN (version 40.01) is a spectral wave model based on the action density balance equation that describes the evolution of two-dimensional wave energy spectra under specified conditions of winds, currents, and bathymetry [2]. The nonstationary mode was employed to simulate time-dependent features of wind-induced waves. For the present simulations, the third-generation mode and the bottom dissipation formulations from Madsen *et al.* [13] with a physical roughness of 0.085 m [14] are used.

The bathymetry is deduced from accurate field surveys and coarser data supplied by Geoscience Australia. A curvilinear computational grid ($76 * 151$ meshes, $153^\circ\ 24'$ E$-153^\circ\ 45'$ E, $28^\circ\ 24'$ S$-27^\circ\ 18'$ S) is implemented with the coarsest meshes around the boundaries. Spatially constant wind, lateral, and offshore wave boundary conditions are provided by the WaveWatch 3 (WW3) grid point, as shown in Fig. 2. Wave outputs are obtained from the Brisbane and Gold Coast seaway buoys and Surfers Paradise Beach (at a 9-m depth).

B. ANNs

ANNs are now generally utilized across diverse fields in science and engineering as a methodology for prediction, estimation, and control. ANNs are generally accepted as a valuable tool for modeling, approximation, and classification [15]–[17]. The common fully interconnected feedforward architecture implements a mapping $\mathbf{y} = f(\mathbf{x}) : \Re^m \rightarrow \Re^n$ and is optimized by providing multiple (assumed noisy) paired samples of the input and target output $\{\mathbf{i}_p \in \Re^m, \mathbf{t}_p \in \Re^n\}$. The transfer function g, which generates a unit's output given net activation from units in the previous layer, should generally be smooth and have a well-bounded range for any input, e.g., $g : (-\infty, \infty) \rightarrow (-1, 1)$. Assuming that the activation function at each layer $i = \{1, \ldots, L\}$ is homogeneous, an ANN implements the function

$$f(\mathbf{x}) = f(\mathbf{a}_0) = h_L\left(h_{L-1}\left(h_{L-\ldots}\left(h_1(\mathbf{a}_0)\right)\right)\right) \tag{1}$$

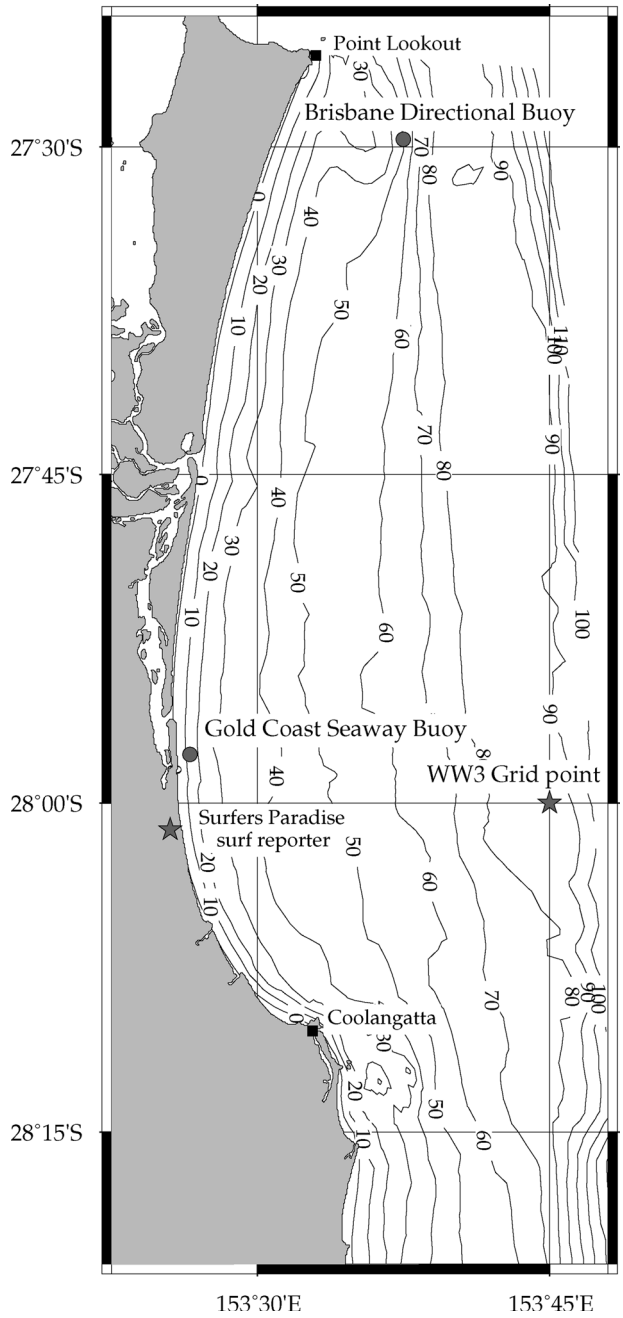

Fig. 2. Geographical area considered in this letter: The nearshore region at the Gold Coast, Australia.

with the layer transformation h defined as

$$\mathbf{a}_i = h_i(\mathbf{a}_{i-1}) = g_i\left(\mathbf{W}_i\left[\mathbf{a}_{i-1}^T\ 1\right]\right) \tag{2}$$

where the set of free parameters (which are termed weights) in the system $\{\mathbf{W}_i\}$ determine the particular nonlinear mapping, noting that $\mathbf{a}_0 = \mathbf{x}$ is an m element vector, $\mathbf{a}_L = \mathbf{y}$ is an n element vector, and necessarily, the dimensions $\{d_i^1, d_i^2\}$ of $\mathbf{W}_i$ have the constraints $d_1^1 = m + 1$, $d_L^2 = n + 1$, and $d_i^1 = d_{i-1}^2$. ANNs are usually conceptualized as a series of neural layers, with forward interconnections between subsequent layers, as shown in Fig. 1.

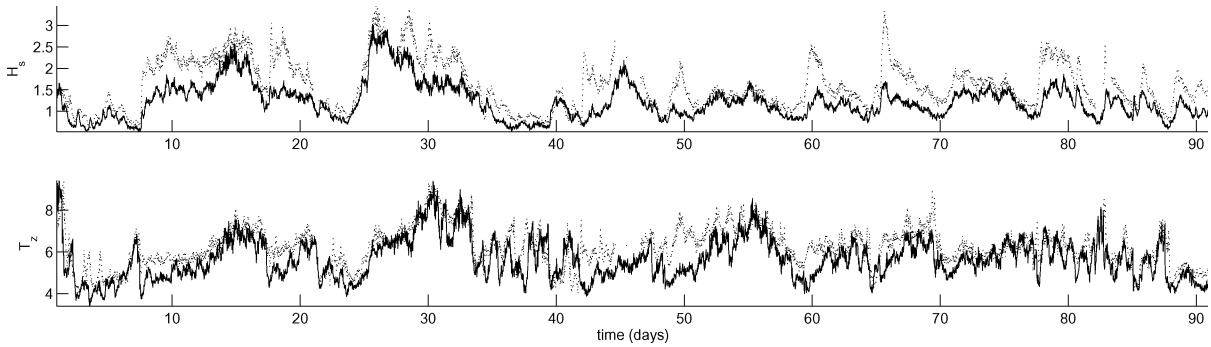

Fig. 3. High temporal resolution (30-min sampling interval) significant wave height H_s and wave period T_z data gathered from the Point Lookout (dotted) and Seaway (solid line) buoys over the time period of the study.

Conventional applications of feedforward networks involve a fixed architecture or topology, with two or three layers L, each having an arbitrary number of neurons (defined by d_i^2). Training a neural network generally involves minimizing the error function $\epsilon_n = \sum_p (\mathbf{y}_p - \mathbf{t}_p)^2$ and utilizing local gradient search algorithms operating on $-\delta\epsilon_n/\delta\{\mathbf{W}_i\}$. Sophisticated and efficient search algorithms, such as the Levenburg–Marquardt method or conjugate gradient descent [18], [19], along with modern computational resources allow for fast optimization of medium-sized networks. Applications of ANNs in a scientific context should take into account the fact that optimization based on local gradients may be expected to yield solutions located in some form of local minima.

II. Data

This letter incorporated global wave model data gathered from NWW3, *in situ* readings from local Environmental Protection Agency (EPA) buoys, and human observations of swell conditions in the nearshore zone from January 1, 2005 to March 31, 2005. The three forms of observations differ significantly in terms of the rate of sampling (with details given later in text), with the buoys representing the highest level of temporal resolution and the human observations representing the lowest. In addition, observations from the three sources occurred on separate time schedules: buoy and NWW3 represented regular sampling, whereas the human observations were sampled on an irregular schedule. Resampling was performed in order to generate a common time index (at 6-h intervals, generating 540 data points). In the case of the human observer and the NWW3 model, this involved upsampling/interpolation and was achieved via determining the value of the exact cubic polynomial fitted to the nearest four (4) sample points at the required time point. In the case of the higher resolution buoy data, downsampling took place using a Gaussian weighted average centered on the desired time point with a bandwidth of $\sigma = 6$ h. This approach also dealt satisfactorily with small regions of missing data that are present (which are less than 2% of the total data). The temporal resolution of the predictive model was necessarily limited by the lowest resolution data stream (that of the human observer). This relatively low sample rate was sufficient for measuring the broad-scale variation in significant wave height, which as shown in Fig. 3 occurred over a time scale of days rather than hours.

TABLE I
Bivariate Correlations Between the NWW3 Input and the Significant Wave Height Targets

NWW3 variable	Surf Rep.	Bris. Buoy	S.W. Buoy
Significant wave height	.54	.73	.72
Primary mean period	.20	-.07	.04
Primary Dir: E	.36	-.11	.08
Primary Dir: N	.25	-.28	-.02
Secondary mean period	.25	.56	.49
Secondary Dir: E	.26	.24	.33
Secondary Dir: N	-.24	-.64	-.48
Wind Wave mean period	.19	-.09	.01
Wind Wave Dir: E	.37	-.15	.05
Wind Wave Dir: N	.09	-.43	-.18
Wind Dir: E	.15	.14	.21
Wind Dir: N	-.18	-.60	-.40
Wind Speed	.20	.56	.48

A. Buoy Data

EPA waverider buoy data from two locations were used in this letter; the locations of these buoys are shown in Fig. 2. Waverider buoys measure wave climate by means of vertical displacement through an accelerometer mounted on a gravity-stabilized platform that is suspended in a fluid-filled plastic sphere. The Gold Coast buoy is located at $27^\circ\ 57.789'$ S latitude and $153^\circ\ 26.523'$ E longitude, with a 15.5-m depth. The Point Lookout buoy is located at $27^\circ\ 29.638'$ S latitude and $153^\circ\ 37.483'$ E longitude. Data were logged at 30-min intervals over the time period of the study. Fig. 3 displays the significant wave height H_s and wave period T_z recorded over the study period.

B. Wave Model (NWW3)

An automated data collection system has been implemented to archive analysis and forecast data from the NWW3 operational wave model [20]. NWW3 uses the output from the National Centres for Environmental Protection Global Forecast System (NCEP GFS) as input for the operational wave models and generates global output on a grid measuring $1^\circ \times 1.25^\circ$ from latitude 78 to -78 $(\times 1^\circ)$ and from longitude 0 to 358.75 $(\times 1.25^\circ)$. Gridded binary output was accessed four times daily at 6-h intervals, extracting wind speed and direction, significant wave height H_s, wind-wave mean period and direction, primary wave mean period and direction,

TABLE II
AVERAGE ESTIMATION PERFORMANCE (FOR ANNS ON A SIXFOLD CROSS-VALIDATION SET)

	Surf Reporter		Gold Coast Seaway Buoy				Brisbane Directional Buoy			
	H_s		H_s		T_z		H_s		T_z	
ANN linear	16.02	*.82*	19.18	*.81*	0.507	*.60*	26.32	*.81*	1.312	*.33*
ANN 3	13.15	*.88*	15.72	*.89*	0.509	*.73*	20.63	*.88*	1.112	*.39*
ANN 5	11.86	*.91*	15.40	*.88*	0.508	*.72*	20.83	*.88*	1.187	*.41*
ANN 7	11.59	*.89*	14.42	*.90*	0.497	*.71*	22.10	*.86*	1.148	*.50*
ANN 9	13.26	*.89*	14.35	*.90*	0.487	*.74*	22.87	*.86*	1.148	*.43*
ANN 11	12.48	*.89*	15.34	*.88*	0.519	*.70*	21.73	*.87*	1.131	*.43*
SWAN	94.42	*.78*	25.10	*.74*	0.949	*.58*	32.09	*.68*	0.869	*.87*
NWW3 H_s	94.10	*.54*	55.28	*.72*			32.64	*.73*		
	SE (cm)	*r*	SE (cm)	*r*	SE (*s*)	*r*	SE (cm)	*r*	SE (*s*)	*r*

and secondary wave mean period and direction. These variables represent a parameterization of the complete directional-wave spectra. In many regions such as Australia, wave parameters are more readily available than full directional-wave spectra.

The data collected at the closest grid point, which is 31.5 km east of Surfers Paradise (28S, 153.75 E), were used as input to the ANNs and as boundary conditions for the nearshore wave model SWAN [2]. So as to avoid discontinuities in the $360^\circ/0^\circ$ region, NWW3 data d in degree format was transformed into a two-element coordinate description $\{n, e\}$ for input to the empirical neural network estimators via $\begin{matrix} n \\ e \end{matrix} = \begin{matrix} \sin \\ \cos \end{matrix} (360^{-1} 2\pi d)$.

C. Beach Observations

Time-stamped recordings were made by visual inspection by a professional surf reporter on location at Surfers Paradise. These estimates of the significant wave height were logged via wireless Internet link. Beach observations were logged at least once a day, in the morning. When significant changes in swell size were observed, a second report was logged in the afternoon.

III. RESULTS

Empirical estimation using the feedforward neural network architecture described in Section I-B was performed using the nine transformed and scaled input variables from NWW3 zero-hour predictions. The target outputs were significant wave heights H_s, as measured by the two wave buoys and the surf reporter. Estimation of the observed wave period T_z, as measured by the two buoys, was also attempted. The available data were partitioned into six sections of equal size (90 data points) for the purpose of sixfold validation. This involved training models using five sections, with testing of model performance on the remaining unseen data. For nonlinear models (i.e., ANNs with a hidden layer), training was repeated using ten random initialization conditions, with the best performing network performance recorded. The process is repeated six times, so that each section is used for testing once. Optimization was halted when performance on the validation set stabilized. The reported results are the average performance over the six sections. Networks varied with respect to the number of hidden neurons. All networks had one hidden layer and used tan-sigmoid and linear transfer functions in the hidden and output layers, respectively. Numerical simulation was carried out using SWAN, and parameters were adjusted several times in order to improve results.

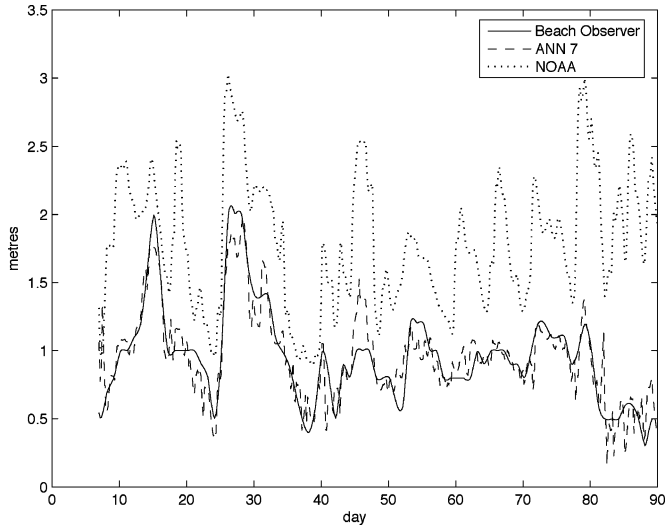

Fig. 4. Significant wave heights at the beach as measured directly by human observer and as predicted by the multilayer feedforward (MLFF) ANN with seven hidden neurons using full NWW3 ocean state variables as input ($SE = 11.59$ cm). Untransformed NWW3 H_s is shown for comparison ($SE = 94$ cm).

Table I displays the bivariate correlations of the NWW3 input variables with the significant wave height recorded at the three locations.

Table II displays the estimation performance in terms of standard error (SE) and normalized correlation coefficient with the target series. The input to all predictive models was the 13 environmental variables provided by the NWW3 system. The rows compare the performance of ANN architectures with variable numbers of hidden neurons with a linear network (equivalent to linear regression). For H_s, the baseline for evaluating performance is represented by the relationship between the readings from NWW3 and the various target series. As the NWW3 model decomposes the swell period into primary, secondary, and wind-driven components, a baseline comparison was not possible for T_z. Fig. 4 displays the best performing ANN for estimation of the surf reporter observations (results for buoys are not plotted in this letter). It should be noted that the ANN output is a concatenation of the six validation sets. Thus, the correspondence in the graph is an indication of performance on unseen data.

IV. Conclusion

From Table II, it may be seen that the baseline NWW3 H_s has a poor correlation with actual H_s measurements at the buoys and beach, with the relationship being weakest for beach-side surf reports. ANNs outperformed the linear regression approach for each prediction task, and generally, the empirical methods were more effective than the numerical modeling using SWAN (apart from estimating T_s at the Brisbane Buoy, where they failed to generalize well). This is not surprising because any theoretical model will be subject to inaccuracies in parameters and survey data. In particular, the current model could have benefited from further calibration, especially in terms of bottom friction. This highlights a significant benefit of empirical prediction, in that good results can be quickly obtained without the need for long development time of simulation and adjusting model parameters.

Estimates of H_s for the surf reporter had a correlation of 0.91 and an SE of 11.86 cm. Although early stopping of training was clearly effective in preventing overlearning, medium-sized networks appeared to generally perform better. This conforms to the ANN theory that a network of complexity comparable to, or slightly more, than the function-mapping problem at hand, produces the best results.

In isolation, the basic ANN method provides little or no insight into the actual physical transformative processes involved. However, it appears to be a powerful approach for approximating the unknown transformation required to estimate local wave properties from a global wind-wave model and has a number of practical applications. From Tables I and II, it is reasonable to suggest that the improvement over baseline in estimation of significant wave height is a result of an approximation of the actual physical transformation as waves move from deep to shallow water. It is unlikely that any single NWW3 parameter can be singled out as the one providing the critical information required for the approximation. However, the local bathymetries would determine which variables were most important. For example, the amount of wave energy that reaches the shore at the surf reporter location in the present study is strongly determined by sheltering from the islands and headlands to the north and south. The bivariate correlations in Table I indicate that the direction of offshore waves affect the amount of energy that reaches the beach. In this form of application, it is not necessarily clear what aspect of the offshore wave climate best predicts nearshore activity. A useful point of view is to make the assumption that observed wave activity at any nearshore location is a deterministic outcome of the interaction between (fixed) local bathymetry and (variable) offshore wave climate. When provided with reasonable estimates of the variable wave climate, it may approximate the transformation required to emulate the modulation effected by local bathymetry. Because any aspect of the offshore wave climate may conceivably affect nearshore measurements, as complete a representation as possible should be exposed to the ANN.

More systematic comparisons of empirical and numerical estimations of nearshore waves have just been completed. We are preparing a report that explains differential ANN performance at several locations in terms of the complexity of the local reflective and diffractive processes using SWAN modeling. Future studies might consider contrasting the use of the full directional-wave spectrum with the (less complete) wave parameters used in the current study. We are currently investigating the potential of using empirical methods to model the nearshore wave transformation at a large number of continental locations for longer time periods. Preliminary results indicate that nonlinear empirical methods provide larger increases in estimation performance at locations where the local bathymetry generates complex wave transformations.

Acknowledgment

Data were obtained with the assistance of D. Robinson and J. Waldron (Australian Environmental Protection Agency's Coastal Services Unit and CoastalWatch Australia).

References

[1] S. N. Londhe and M. C. Deo, "Artificial neural networks for wave propagation," *J. Coastal Res.*, vol. 20, no. 4, pp. 1061–1070, 2004.

[2] N. Booij, R. Ris, and L. Holthuijsen, "A third-generation wave model for coastal regions—I: Model description and validation," *J. Geophys. Res.*, vol. 104, no. C4, pp. 7649–7666, 1999.

[3] P. D. Komar and M. K. Gaughan, "Airy wave theory and breaker height prediction," in *Proc. 13th Conf. Coastal Eng.*, 1972, pp. 405–418.

[4] P. C. Caldwell, "An empirical method for estimating surf heights from deep water significant wave heights and peak periods in coastal zones with narrow shelves, steep bottom slopes, and high refraction," presented at the 8th Int. Workshop Wave Hindcasting Forecasting, Nov. 14–19, 2004.

[5] M. C. Deo and S. S. Jagdale, "Prediction of breaking waves with neural networks," *Ocean Eng.*, vol. 30, no. 9, pp. 1163–1178, Jun. 2003.

[6] O. Makarynskyy, A. Pires-Silva, D. Makarynska, and C. Ventura-Soares, "Artificial neural networks in wave predictions at the west coast of Portugal," *Comput. Geosci.*, vol. 31, no. 4, pp. 415–424, 2005.

[7] M. C. Deo, A. Jha, A. S. Chaphekar, and K. Ravikant, "Neural networks for wave forecasting," *Ocean Eng.*, vol. 28, no. 7, pp. 889–898, Jul. 2001.

[8] J. D. Agrawal and M. Deo, "Online wave prediction," *Marine Struct.*, vol. 15, no. 1, pp. 57–74, 2002.

[9] C. E. Balas, L. Koc, and L. Balas, "Predictions of missing wave data by recurrent neuronets," *J. Waterw. Port Coast. Ocean Eng.*, vol. 30, no. 5, pp. 256–265, Sep./Oct. 2004.

[10] R. Kalra, M. Deo, R. Kumar, and V. K. Agarwal, "Artificial neural network to translate offshore satellite wave data to coastal locations," *Ocean Eng.*, vol. 32, no. 16, pp. 1917–1932, Nov. 2005.

[11] O. Makarynskyy, "Improving wave predictions with artificial neural networks," *Ocean Eng.*, vol. 31, no. 5/6, pp. 709–724, Apr. 2004.

[12] J. R. Medina, "Improving wave predictions with artificial neural networks, by O. Makarynskyy," *Ocean Eng.*, vol. 32, no. 1, pp. 101–103, Jan. 2005.

[13] O. Madsen, Y. Poon, and H. Graber, "Spectral wave attenuation by bottom friction: Theory," in *Proc. 21st Int. Conf. Coastal Eng.*, 1988, pp. 492–504.

[14] B. Castelle, P. Bonneton, N. Senechal, H. Dupuis, R. Butel, and D. Michel, "Dynamics of wave-induced currents over an alongshore non-uniform multiple-barred sandy beach on the Aquitanian Coast, France," *Cont. Shelf Res.*, vol. 26, no. 1, pp. 113–131, Jan. 2006.

[15] F. M. H. I. Kostanic, *Principles of Neurocomputing for Science and Engineering*. New York: McGraw Hill, 2001.

[16] C. Bishop, *Neural Networks for Pattern Recognition*. Oxford, U.K.: Clarendon, 1995.

[17] B. D. Ripley, *Pattern Classification and Neural Networks*. Cambridge, U.K: Cambridge Univ. Press, 1996.

[18] D. Marquardt, "An algorithm for least-squares estimation of nonlinear parameters," *SIAM J. Appl. Math.*, vol. 11, no. 2, pp. 431–441, Jun. 1963.

[19] A. R. Kan and G. Timmer, *Global Optimization: A Survey, International Series of Numerical Mathematics*. Basel, Switzerland: Birkhauser Verlag, 1989.

[20] H. L. Tolman, "User Manual and System Documentation of Wavewatch-III Version 1.18," NOAA / NWS / NCEP / OMB, Tech. Rep. 166, 1999.